Asian Journal of Pharmaceutical Sciences 15 (2020) 365–373

Available online at www.sciencedirect.com

ScienceDirect

journal homepage: www.elsevier.com/locate/AJPS

Original Research Paper

Arsenic trioxide encapsulated liposomes prepared via copper acetate gradient loading method and its antitumor efficiency

Shaoning Wang[a], *Chunxiu Liu*[b], *Cunyang Wang*[a], *Jia Ma*[a], *Hui Xu*[b,*], *Jianbo Guo*[c], *Yihui Deng*[b]

[a] *School of Pharmaceutical Engineering, Shenyang Pharmaceutical University, Benxi 117004, China*
[b] *School of Pharmacy, Shenyang Pharmaceutical University, China*
[c] *Shanxi Institute for Food and Drug Control, Xi'an 710065, China*

ARTICLE INFO

Article history:
Received 28 June 2018
Revised 4 November 2018
Accepted 4 December 2018
Available online 19 December 2018

Keywords:
Arsenic trioxide
Liposomes
Copper acetate gradient
Pharmacokinetics
Tissue distribution
Antitumor activity

ABSTRACT

In this study, arsenic trioxide (ATO) was encapsulated in liposomes via copper acetate ($Cu(OAc)_2$) gradients and high entrapment efficiency of over 80% was obtained. The average particle size and the zeta-potential of the liposomes were detected to be 115.1 ± 29.1 nm and −21.97 ± 0.6 mV, respectively. The TEM images showed rod-like precipitates in the inner aqueous phase, which was supposed be due to the formation of insoluble ATO–Cu complex. The *in vitro* drug release of ATO–Cu liposomes exhibited a sustained release over 72 h, and the release rates decreased with the increase of the pH of release media. Pharmacokinetic and tissue distribution studies of ATO liposomes showed significantly reduced plasma clearance rate, increased AUC_{0-12h} and $T_{1/2}$, and improved tumor distribution of As compared to *iv* administration of ATO solution. The anti-tumor effect of ATO loaded liposomes to S180 tumor-bearing mice was significantly improved with a tumor inhibition rate of 61.2%, meanwhile the toxicity of encapsulated ATO was greatly decreased. In conclusion, ATO can be effectively encapsulated into liposomes by remote loading method via $Cu(OAc)_2$ gradients; the co-administration of ATO and Cu(II) via liposomal formulation may find wide applications in the treatment of various tumors.

1. Introduction

Arsenic trioxide (As_2O_3, ATO) is a successfully developed therapeutic agent used for the treatment of acute promyelocytic leukemia [1,2]. Preclinical studies have also shown the antitumor activity of ATO in murine solid tumor models, including breast, brain, liver, renal, and bladder cancers [3,4]. Unfortunately, little or even no antitumor

* Corresponding author. School of Pharmacy, Shenyang Pharmaceutical University, No. 26 Huatuo Road, High & New Technology Development Zone, Benxi 117004, China. Tel.: +86 24 43520550.
E-mail address: xuhui_lab@163.com (H. Xu).
Peer review under responsibility of Shenyang Pharmaceutical University.

https://doi.org/10.1016/j.ajps.2018.12.002

efficacy has been observed in clinical trials for the treatment of solid tumors with ATO [5]. Two factors seem to be the limitation for the applications of ATO in clinical practice, i.e. rapid renal clearance that greatly limits tumor uptake of ATO, and dose-limiting toxicity [6,7]. Dose of more than 0.20 mg ATO/kg/d may cause severe side effect, including flaccid paralysis and renal failure [8].

Liposomal carriers have been intensively investigated to deliver active drugs to tumor, maintain drug stability, and prolong blood circulation period, thus improve antitumor efficiency and reduce unexpected side effects of the therapeutic agents [9,10]. Encapsulation of ATO in liposomes may alter its tissue distribution in a beneficial way. However, previous attempts demonstrated that ATO liposomes were unstable due to the rapid diffusion of $As(OH)_3$ through liposomal lipid bilayer [11]. In fact, many liposomal formulations showed the drawback of rapid drug release, such as ciprofloxacin and vincristine liposomes [12,13], and different strategies were introduced to solute this problems depending on the properties of encapsulated agents.

The precipitation of drug with the transitional metal ion (Cu^{2+}, Ni^{2+}, Mn^{2+}, etc.) in the preformed liposomes was proved to be effective in retaining drug molecular inside liposomes during blood circulation [14–16]. ATO was effectively loaded into liposome by precipitating with nickel (II) inside the inner aqueous phase, which showed therapeutic potential to solid tumors in animal models [17–19].Different to nickel, copper (Cu) is an essential trace element in human body, which plays important roles in regulating the physiological functions of circulation, excretion, respiration, digestion and nerve system.In addition, recent studies also found unique role of copper in the treatment of various tumors. Wang et al. reported that Cu(II) liposomes exhibit low toxicity but high tumor inhibition rate to prostate cancer [20]. Combined administration of disulfiram and Cu(II) resulted in significant therapeutic effects to prostate cancer and glioblastoma cancer [21,22]. In another study, Cu(II) coordination complexes were reported to inhibit DNA synthesis and induce cell death of multiple cancer cell types with reduced toxicity to normal cells, which was expected to be the potential anticancer agents in replacement of platinum [23]. Recently, Zhou [24] et al. reported that poly(metal) containing As (III) and Cu (II) significantly induced the apoptosis and autophagy of K562 leukemia cells and HepG2 cells.

In this study, ATO and Cu(II) was co-loaded into liposomes using a remote loading method through copper-acetate ($Cu(OAC)_2$) gradient aiming to obtain higher ATO encapsulation efficiency and better antitumor activity. The *in vitro* drug release, pharmacokinetics and tissue distribution properties of the liposomes were evaluated, and the antitumor efficacy was studied in S180 tumor-bearing mouse model.

2. Materials and methods

2.1. Materials, cell line, and animals

Sodium arsenite (purity > 98.0%) was purchased from Xiya Reagent (Chengdu, China). Hydrogenated soy phosphatidylcholine (HSPC) and N-(carbonyl methoxypolyethyleneglycol 2000)-1,2-distearoyl-sn-glycero-3-phosphoethanolamine (mPEG2000-DSPE) were purchased from Avanti Polar Lipid, Inc. (Alabama, USA). Cholesterol (CH) was obtained from China National Medicines Corporation Ltd (Shanghai, China). Sephadex G-50 was obtained from Sigma-Aldrich (German). All other chemicals used were of analytical or chromatographic grade.

Murine sarcoma S180 cell line was purchased from the Cell Bank of the Chinese Academy of Sciences (Shanghai, China).

Wistar rats weighing 180–220 g (7–8 weeks) and male Kunming mice weighing 18–22 g (6–7 weeks) were obtained from the Experimental Animal Center of Shenyang Pharmaceutical University (Shenyang, China). All animal care and experiments were carried out in accordance with the Guidelines of the Animal Welfare Committee of Shenyang Pharmaceutical University.

2.2. Preparation of ATO liposomes

Three loading procedures were introduced to encapsulate ATO into liposomes, i.e., modified ethanol injection method, pH gradient method and $Cu(OAc)_2$ gradient method, as described below.

Modified ethanol injection method: HSPC, CH, and DSPE-PEG2000 (3/1/1, w/w) were dissolved in absolute ethanol, after the large portion of ethanol was removed at 65 °C, ATO aqueous solution (200 mM, pH 7.4) was added to hydrate the lipid mixture. The resulting liposomal suspension was ultrasonicated with a JY92-2D Vibra-cell probe-sonicator (Scientz Biotechnology Co, Ltd., Ningbo, China) and then extruded through polycarbonate membrane of 0.2 μm pore size to yield unilamellar ATO liposomes.

pH gradient method: HSPC, CH, and DSPE-PEG2000 (3/1/1, w/w) were dissolved in absolute ethanol, after the large portion of ethanol was removed at 65 °C, citric acid buffer (300 mM, pH 4.3) was added to hydrate the lipid mixture. The resulted blank liposomal suspension was ultrasonicated and extruded through polycarbonate membrane of 0.2 μm pore size to yield unilamellar blank liposomes. Sodium phosphate solution (500 mM) was added to adjust the pH of the external solution to 7.4 and generate transmembrane pH gradient. The gradient liposomal suspension was then mixed with ATO aqueous solution (100 mM, pH 7.4) with a volume ratio of 1:1, and incubated at 60 °C for 10 min for drug loading.

$Cu(OAc)_2$ gradient method: HSPC, CH, and DSPE-PEG2000 (3/1/1, w/w) were dissolved in absolute ethanol, after the large portion of ethanol was removed at 65 °C, $Cu(OAc)_2$ aqueous solution was added to hydrate the lipid mixture. The resulted blank liposomal suspension was ultrasonicated and extruded through polycarbonate membrane of 0.2 μm pore size to yield unilamellar $Cu(OAc)_2$ liposomes. The $Cu(OAc)_2$ gradient liposomes (Cu-L) were formed by passing through a micro column packed with cation-exchange fiber or Sephadex G-50 micro-column, and then the pH of the external aqueous phase was adjusted to different pH with Na_3PO_4 solution (300 mM). The gradient liposomal suspension was mixed with ATO aqueous solution (100 mM, pH 7.4) with a volume ratio of 1:1, and incubated at 60 °C for 10 min for drug loading.

Un-encapsulated ATO was removed by passing the liposomal suspension through the column packed with

Sephadex G-50. The amount of ATO encapsulated in the liposomes was then measured with an ICPE-9000 inductively coupled plasma optical emission spectrometer (ICP-OES, Shimadzu, Japan). The encapsulation efficiency (EE) was then calculated as EE% = (actual amount of the drug encapsulated in liposomes) / (initial amount of the drug added) × 100.

2.3. Characterization to the liposomes

Particle size and zeta potential of the liposomes were determined using a NICOMP 380 HPL Submicron Particle Analyzer (Particle Sizing System, CA) after the dilution of liposomes with deionized water.

The TEM images of the liposomes were captured using a JM-1200EX transmission electron microscopy (TEM, JEOL Ltd., Japan). Briefly, a diluted suspension of liposomes was dropped on formvar-coated copper grids and stained with phosphotungstic acid solution (2%, w/v). The stained sample was allowed to dry in air before observation.

2.4. In vitro drug release

ATO liposomes (ATO–Cu-L, 2 ml) prepared by $Cu(OAc)_2$ gradient method or ATO solution (ATO-S) was transferred into dialysis tubes (Cut-off MW: 8000–12 000, Millipore, USA), which were immersed into 100 ml of PBS (0.05 M) of pH 5.0, 6.5 and 7.4 at 37 °C with constant stirring. At specific time intervals, 5 ml of release media was withdrawn and replaced with fresh media. The ATO concentrations were determined by ICP-OES.

2.5. Pharmacokinetics

Six Wistar rats were randomly divided into two groups ($n = 3$), each group received single intravenous administration of ATO–Cu-L or ATO-S via the tail vein. Blood samples were collected into heperinzied tubes from the retro-orbital sinus at 0.017 h, 0.083 h, 0.25 h, 0.5 h, 1 h, 2 h, 4 h, 8 h and 12 h, respectively. The blood samples were centrifuged (4000 r/min, 5 min), and 0.25 ml plasma was collected into the PTFE tubes. Then 5 ml nitric acid and 2 ml hydrogen peroxide were added. Samples were digested by the microwave reaction system (CEM Mars 6, USA). Then the digested solutions were kept at 130 °C to remove acidic solution. The residual solution was re-dissolved by 2% nitric acid solution for ICP-EOS analysis. The pharmacokinetic parameters were calculated using DAS 2.0 software (the net for drug evaluation of China).

2.6. Tissue distribution

Xenografted S180 tumor bearing mice were used to evaluate the tissue distribution of elemental As after i.v. administration of ATO–Cu-L and ATO-S. Tumors were xenografted by injecting S180 cells (1.8×10^7 cells per mouse) subcutaneously into the right axillary flank of male Kunming mice. Nine days after inoculation, the mice received single administration of either ATO–Cu-L or ATO-S via tail vein at a dose of 3 mg As/kg body weight. At predetermined intervals, mice were sacrificed at 0.083 h, 0.5 h, 1 h, 6 h and 12 h after treatment. The livers, lungs, kidneys and tumors were collected and treated as described in 2.5. *Pharmacokinetics* for ICP-OES analysis of As levels.

Table 1 – The encapsulation efficiency of ATO liposomes prepared with different drug loading methods.

Loading methods		$Cu(OAc)_2$(mmol/l)	EE (%)
Passive loading	Ethanol injection		21.3 ± 1.4
Remote loading	pH gradients		28.4 ± 1.5
	$Cu(OAc)_2$ gradients[1,*]	100	56.8 ± 1.2
	$Cu(OAc)_2$ gradients[1,*]	200	82.0 ± 1.8
	$Cu(OAc)_2$ gradients[1,*]	300	83.5 ± 0.7
	$Cu(OAc)_2$ gradients[2,*]	200	83.1 ± 1.6

[1] $Cu(OAc)_2$ gradient was generated via passing through cation exchange fiber;
[2] $Cu(OAc)_2$ gradient was generated via passing through Sephadex G-50 micro-column;
* The pH of the external aqueous phase was adjusted to 7.

2.7. Antitumor efficacy and toxicity of liposomes

The antitumor activities of ATO–Cu-L to tumor bearing mouse model were evaluated. After tumor inoculation, the mice were randomly divided into four groups ($n = 6$) and intravenously treated with normal saline (0.9% NaCl, control), $Cu(OAc)_2$ solution (Cu-S, 3.5 mg Cu/kg), Cu-L (3.5 mg Cu/kg), ATO-S (3 mg As/kg), and ATO–Cu-L (3 mg As/kg, 3.5 mg Cu/kg), respectively. All mice were treated with different formulations through the tail vein injection at the 3rd, 6th, 9th and 12th day after inoculation. Mice were weighed on the day of tumor inoculation, and their weights were recorded every two days. Tumor sizes were measured with a caliper and calculated as $[(\text{major axis}) \times (\text{minor axis})^2]/2$. At day 14, the animals were sacrificed, and the tumors were weighted and the mass inhibition rate (%) was calculated with the equation: mass inhibition rate $(\%) = [(W_c\text{-}W_T)/W_c] \times 100\%$, where W_c is the average tumor weight of control group, W_t is the average tumor weight of treated group. Kidneys were fixed with 4% formaldehyde, embedded in paraffin, and cut into slices with a thickness of 6 μm. The sections were stained with hematoxylin and eosin (H&E), and observed under BA300 Pol. Microscope (Motic Ins., Xiamen, China).

2.8. Statistical analysis

All data were expressed as the mean ± standard deviation (SD). Statistical comparisons were analyzed by using a two-tailed Student's *T*-test for the two groups, in all cases, $P < 0.05$ was considered statistically significant.

3. Results and discussion

3.1. Encapsulation of ATO into liposomes

Table 1 summarized the encapsulation efficiency (EE) of ATO liposomes prepared with different drug loading methods. Compared to the ethanol injection method (EE: 21.3% ± 1.4%)

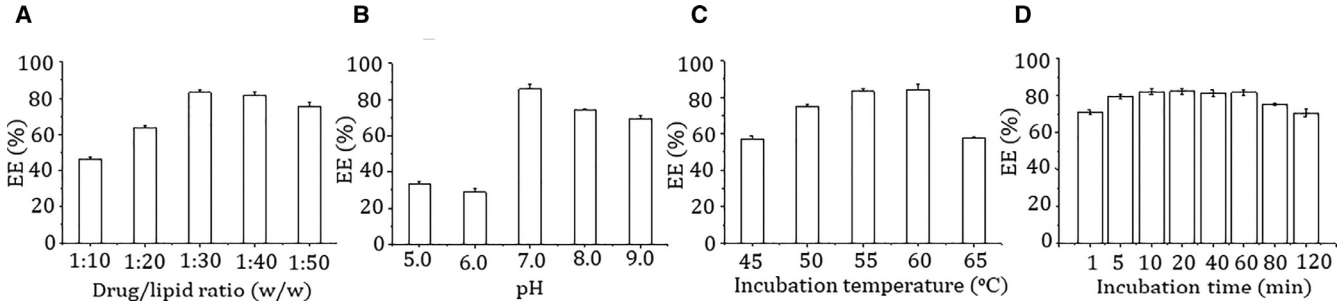

Fig. 1 – Effect of drug/lipid ratio (A) pH of exterior aqueous phase (B) incubation temperature (C) and time (D) on the encapsulation efficiency of ATO.

or the pH-gradient method (EE: 28.4% ± 1.5%), the trans-liposomal $Cu(OAc)_2$ gradients obviously assisted drug encapsulation, and EE of 56.8% ± 1.2% was obtained at the $Cu(OAc)_2$ concentration of 100 mmol/L, even more than 80% was obtained at higher $Cu(OAc)_2$ concentrations of 200 mmol/L and 300 mmol/L. As shown in Table 1, when the $Cu(OAc)_2$ gradientswere formed by passing liposomes through cation exchange fiber or Sephadex G-50 micro-column, the EE values of ATO liposomes have no difference ($P > 0.1$), which were 82.0% ± 1.8% and 83.1% ± 1.6%, respectively.

The drug/lipid ratio, pH of external aqueous phase, incubation temperature and time, might be the key factors that affect the remote loading of ATO into liposomes. The drug/lipid ratio is generally one of the most important factors. Fig. 1A showed that the EE increased with the decrease of drug/lipid ratio from 1:10 to 1:30, while further decrease of the drug/lipid ratio did not affect the EE obviously. The pH of external aqueous phase also had great influence on the EE of ATO (Fig. 1B). At pH 5 and 6, the EE was only about 30%, the maximum EE was achieved to be 85.8% ± 2.3% at pH 7.0, and then decreased to about 74.2% ± 0.7% and 69.2% ± 1.6% at higher pH of 8 and 9. The present results also indicated certain temperature dependent drug loading process. As shown in Fig. 1C, the highest EE was obtained at incubation temperature of 55 °C and 60 °C (83.2% ± 1.3% and 84.0% ± 3.3%, respectively), higher or lower temperatures both resulted into decreased drug entrapment. According to Fig. 1D, the incubation time had no obvious influence on drug entrapment. The EE reached the maximum at 10 min incubation, and extended incubation time had no further benefit to drug loading, the EEs even decreased slightly after incubation more than 60 min.

The ATO–Cu-L suspension was turbid liquid with opalescence appearance and light green-blue color (Fig. 2A, right), which was different to the slight blue color of $Cu(OAc)_2$ gradient liposomes (Fig. 2A, left). This result indicated the possibility of new form ATO–Cu complex in the inner aqueous phase instead of the soluble Cu(II) form in the $Cu(OAc)_2$ gradient liposomes. Under the transmission electron microscope, the prepared liposomes were sphere-like, small unilamellar vesicles with a diameter of about 100 nm (Fig. 2B), which was in accordance with that determined by NICOMP 380 HPL Submicron Particle Analyzer (115.1 ± 29.1 nm, Fig. 2C) . Meanwhile, rodlike precipitates inside the inner phase was observed, which was believed to be of insoluble ATO–Cu complex formed in inner aqueous phase during the remote loading process. The *zeta*-potential of ATO–Cu-L was also detected to be −21.97 ± 0.6 mV (Fig. 2D).

Due to the rapid clearance of ATO, low tumor targeting efficiency, poor therapeutic efficacy at low doses and severe systemic toxicity at high dose, ATO gained less success in clinical practice in cancer therapy except for acute promyelocytic leukemia (APL) [25]. Encapsulation of chemotherapeutic agents in liposomes has got great success in modifying the *in vivo* fates of drugs, thus improving their antitumor efficacy and decreasing the side effects, such as doxorubicin liposomes (Doxil®), irinotecan liposomes (Onivyde®), etc. [26]. As a small inorganic molecular substance, the ATO loaded liposomes prepared by passive loading method showed a very low encapsulation efficiency and poor stability [11]. For instance, in this study, the EE value of only about 20% was obtained by the modified ethanol injection method. In order to increase the EE of ATO, a remote loading method via transmembrane $Cu(OAc)_2$ gradients was introduced, and high EE value of over 80% was obtained.

For the increased encapsulation of ATO, two factors are believed to play important roles, one is the formation of insoluble ATO–Cu complex, and the second is the formation of transmembrane OAc^- gradient. As illustrated in Fig. 3, at neutral pH, the predominant portion of ATO ($As(OH)_3$, $pKa_1 = 9.3$) was electro-neutral, which is readily to permeate across the liposomal bilayers [27]. After entering the inner aqueous phase containing $Cu(OAc)_2$, the insoluble ATO–Cu complex may precipitate and reside inside the inner aqueous phase of the liposomes, at the same time the liberated proton associates with $OAc^-$to form HOAc which will tend to diffuse out of the liposomes. In this study,the cation exchange fiber and Sephadex G-50 micro-column were used to form the transmembrane gradient separately depending on their different separation mechanisms.After passing liposomes through Sephadex G-50 micro-column, both Cu^{2+} gradients and OAc^- gradients were formed at the same time. On the contrary, after passing the liposomes through the cation exchange fiber, OAc^- was still remained in the extraliposomal medium, and only Cu^{2+} gradient was established. An interesting finding was that there was no difference on the EE values of ATO liposomes, irrespectively to the methods used to form the gradient (Table 1). This result indicated that OAc^- gradient was not the key driving

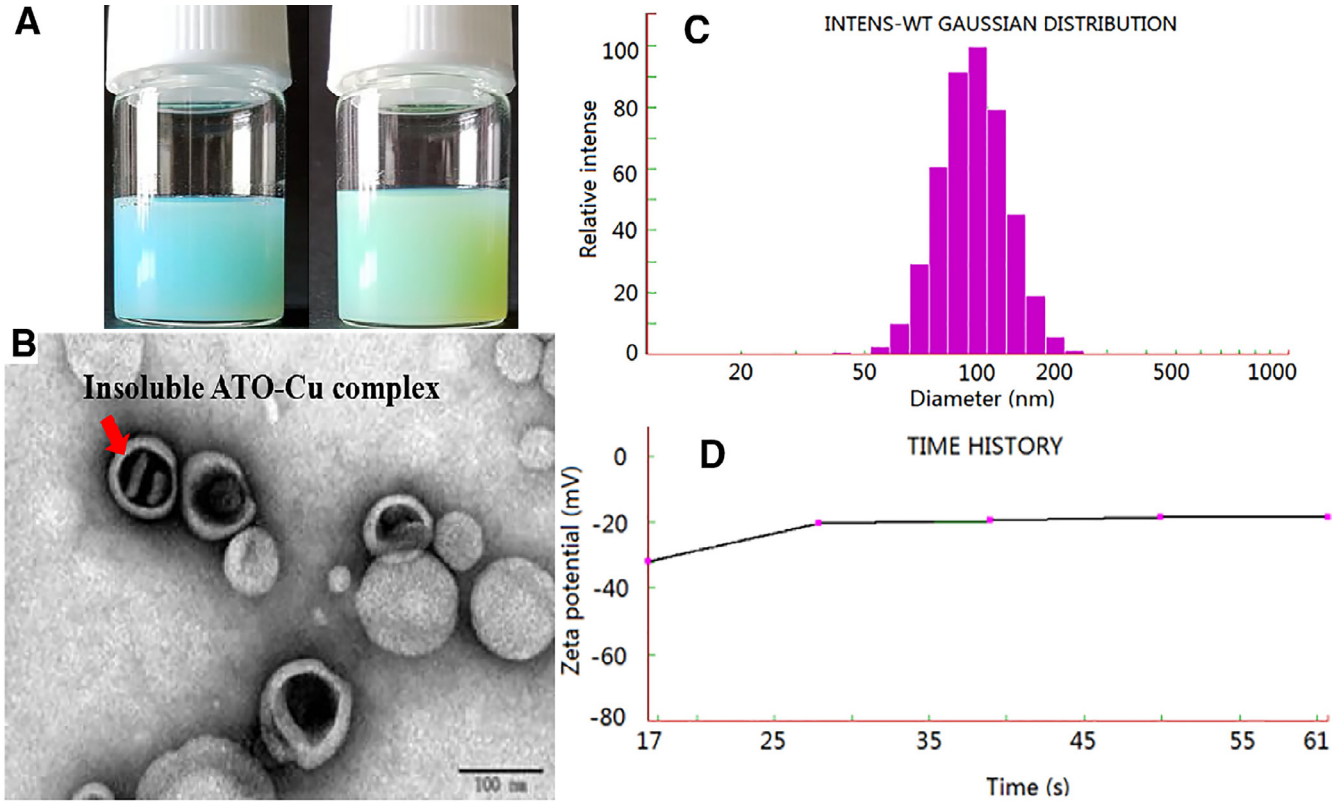

Fig. 2 – The characteristics of liposomes. (A)The appearance of $Cu(OAc)_2$ grandient liposomes (left) and ATO–Cu-L liposomes (right); (B) the TEM imageof ATO–Cu-L liposomes; (C) Particle size distribution of ATO–Cu-L liposomes; and (D) Time history curve of zeta potential.

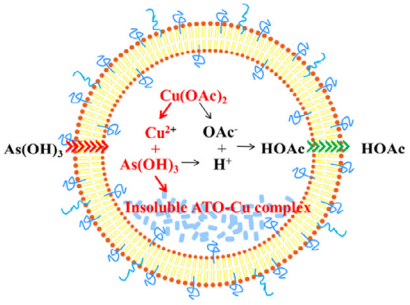

Fig. 3 – Schematic illustration of ATO loading mechanism into liposomes via $Cu(OAc)_2$ gradient.

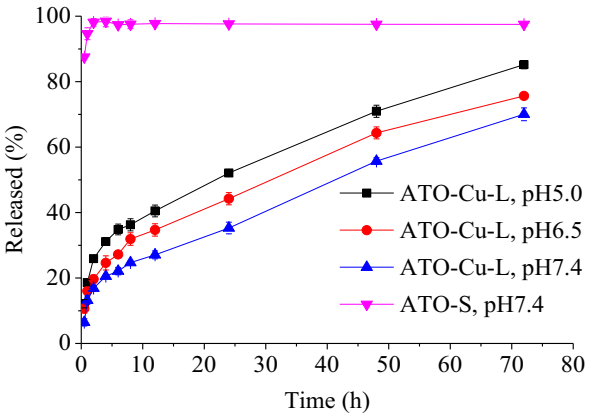

Fig. 4 – *In vitro* release profiles of ATO–Cu -L and ATO-S in PBS.

force for the encapsulation of ATO, while the formation of insoluble ATO–Cu complex (Fig. 2B) may be the main reason for high ATO encapsulation (Fig. 3). Furthermore, good stability of ATO in liposome could also be attributed to such ATO–Cu complex formation, and due to the same reason the liberation of ATO from liposomes was obviously delayed as shown in Fig. 4.

3.2. *In vitro release*

Retention of active drugs in liposomes was the prerequisite for prolonged *in vivo* circulation and effective antitumor efficacy. *In vitro* release test of the liposomal formulations was performed in PBS of different pH to evaluate the retention ability of ATO inside liposomes. As shown in Fig. 4, free ATO completely diffused out of the dialysis tube within 1 h. On the contrary, only 13% of the ATO released from the ATO–Cu-L at the first 1 h, followed by slow release lasted over 72 h. The drug release of ATO–Cu-L also showed obvious pH-dependent pattern, the release rates decreased with the increasing of medium pH, which indicated that the ATO–Cu complex that embedded inside liposomal interior aqueous phase could

Table 2 – The tumor inhibition rates of various formulations ($n = 3–6$).

Treatment group	Number of death	Weight of tumor (g)	Inhibition ratio(%)	P_1	P_2	P_3	P_4
Saline	1	5.23 ± 0.54	/	/	/	/	/
Cu-S	0	4.35 ± 0.23	16.5	<0.05	/	/	/
Cu-L	0	3.55 ± 0.17	32.1	<0.05	<0.05	/	/
ATO-S	3	3.31 ± 0.15	36.7	<0.05	/	/	
ATO–Cu-L	0	2.02 ± 0.08	61.2	<0.05	<0.05	<0.05	<0.05

P_1: compared to normal saline group; P_2: compared to Cu-S group; P_3: compared to Cu-L group; P_4: compared to ATO-S group.

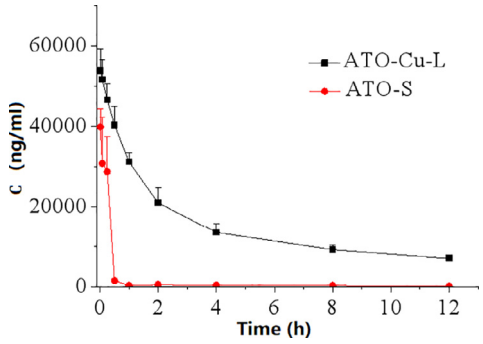

Fig. 5 – Plasma As concentration-time curves after iv administration of ATO–Cu-L and ATO-S ($n = 3$).

slowly dissolve under neutral conditions, but readily dissolve in acidic medium.

3.3. *Phamacokinetics*

Fig. 5 showed the plasma levels of elemental As *versus* time curves after *i.v.* administration of ATO–Cu-L and ATO-S to rats. Compared to ATO-S, encapsulation of ATO in liposomes resulted in dramatically altered plasma concentration *versus* time profile characterized by greatly prolonged blood circulation period. According to Table 2, the plasma half-life ($T_{1/2}$) of ATO–Cu-L extended from 3.08 ± 0.66 h to 7.01 ± 0.77 h ($P < 0.05$), and the AUC0-12 h increased from 15 093.66 ± 1565.20 μg·h/l to 248 538.53 ± 16 069.90 μg·h/l ($P < 0.05$), when compared to ATO-S.

The prolonged circulation period of liposomal ATO as shown in Fig. 5 could be attributed to the firm encapsulation of ATO, as well as the pegylated surface of ATO–Cu-L. As one of the main lipid bilayer ingredients, the incorporation of mPEG2000-DSPE greatly improved the steric stability of the liposomes, and the PEG chains that stretched out on the surface of liposomes was intensively reported to be able to prolong the blood circulation of nano-sized drug carriers [28]. Meanwhile, with the increased exposure time in circulation, the liposomes tend to accumulate in tumor due to the enhanced permeability and retention (EPR) effect [29,30].

3.4. *Tissue distribution*

The tissue distribution of As were evaluated after *i.v.* administration of ATO–Cu-L and ATO-S to tumor-bearing mice. Fig. 6 indicated that the accumulation of As in tumors was obviously enhanced after i.v. administration of ATO–Cu-L to mice, which was about 2 times higher than that of ATO-S group (Fig. 6). Meanwhile, ATO–Cu-L showed delayed peak time of As from 5 min (ATO-S) to 30 min, as well as decreased accumulation of As in liver and kidney.

The distribution of As after i.v. administration of ATO–Cu-L (about 110 nm) was significantly enriched in tumor compared to that of ATO-S (Fig. 6), and thus improved the tumor inhibition rate (Table 2).

3.5. *Antitumor activity*

The *in vivo* antitumor efficacy of ATO–Cu-Lwas evaluated in a xenografted S180 tumor bearing mouse model. The tumor growth profiles (Fig. 7A) demonstrated that both ATO formulations and Cu(II) formulations showed inhibition to tumor growth of different extent compared to the control group (Normal saline). It is worth to notice that the tumor growth of the mice treated with ATO–Cu-L was almost completely inhibited and the tumor volumes remained at about 700 mm^3 with no further increase after 8 days of inoculation. At day 14, the animals were sacrificed, the tumors were weighted. The number of mice dead, the tumor weight and tumor inhibition rate(%) were listed in Table 2, and the morphologies of tumors were shown in Fig. 7B. In this study, Cu(II) alone also displayed certain antitumor activity, with an inhibition rate of 16.5% ± 4.3% and 32.1% ± 7.6% for Cu-S and Cu-L, respectively. ATO-S showed similar tumor inhibition rate to that of Cu-L ($P > 0.1$), the inhibition rate of ATO was increased to 62.1% ± 1.6% ($P < 0.05$), when ATO and Cu(II) were co-administrated via the liposomal formulation (ATO–Cu-L).

3.6. *Toxicity evaluation*

Weight loss of mice was usually used to reflect the toxicity of the chemotherapeutic treatment to animals [31]. In this study, no obvious decrease of mice body weight of all groups was observed, also there was no obvious differences of body weight between drug treated and control group was found (Fig. 8A). However, 3 mice of ATO-S group died during the treatment process, which proved the higher toxicity of free ATO as reported in literature [8].

The low toxicity of liposomal formulation could be attributed to the changed *in vivo* fate of ATO–Cu-L including

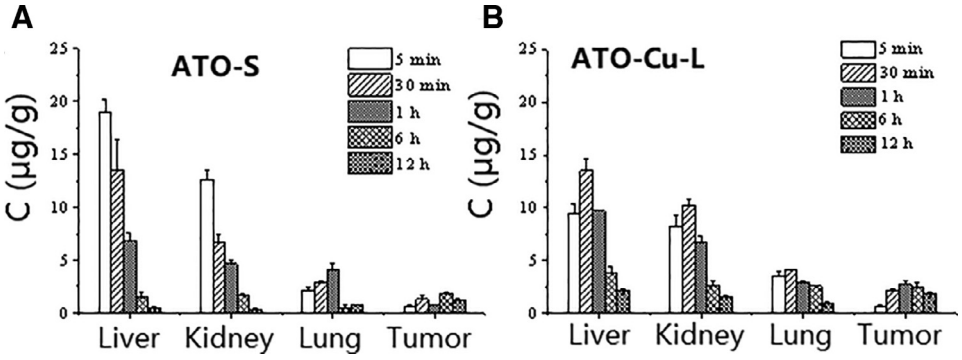

Fig. 6 – Tissue As concentration-time relationship after i.v. administration of ATO-S (A) and ATO–Cu -L (B) to mice ($n = 3$).

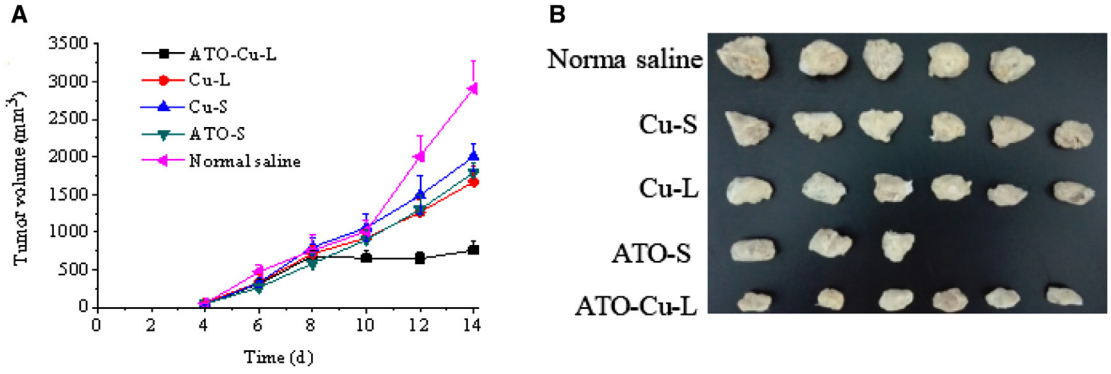

Fig. 7 – Tumor growth curves of S-180 bearing mice intravenously injected with ATO–Cu-L, ATO-S, Cu-L, Cu-S and normal saline (A) and the photographs of tumors of different experiment groups at day 14 after inoculation (B). Results presented as mean ± SD ($n = 3–6$).

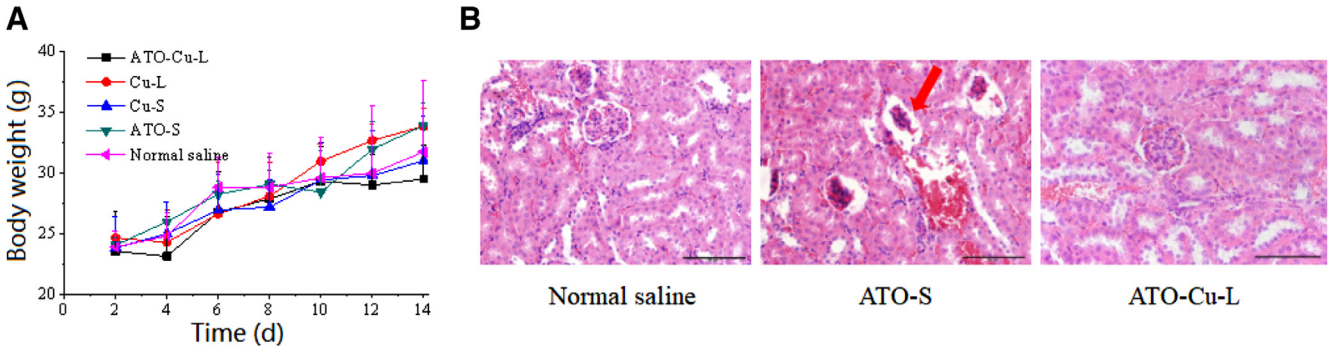

Fig. 8 – Primary evaluation of the toxicity of ATO–Cu-L. (A)Body weight changes of S180 tumor bearing mice injected with ATO–Cu-L, ATO-S, Cu-L, Cu-S and normal saline (n = 3–6). (B) The renal histopathology stained with hematoxylin and eosin (H&E) of tumor bearing mice treated with normal saline, ATO-S, and ATO–Cu-L. Scale bar = 50 μm.

less distribution of As in liver and kidney. Due to its predominant renal clearance mechanism and possible renal failure caused by ATO, the renal histopathology of mice was studied after the treatment with normal saline, ATO-S, and ATO–Cu-L. As shown in Fig. 8B, the renal histopathology of ATO-S group exhibited atrophied glomeruli, while no damage to renal histopathology was found in ATO–Cu-L group, although the same dose regime of As was administrated to both groups.

4. Conclusion

In conclusion, $Cu(OAc)_2$ gradient mediated loading method was successfully used to encapsulate ATO into liposomes with high encapsulation efficiency. The ATO loaded liposomes showed sustained and pH-dependent *in vitro* release properties. Pharmacokinetic and tissue distribution studies of liposomes indicated significantly reduced plasma clearance

rate, increased $AUC_{0\text{-}12h}$ and half-life, and improved tumor distribution of As compared to *i.v.* administration of ATO solution. More importantly, the ATO loaded liposomes improved the anti-tumor effect and decreased the toxicity in S180 tumor bearing mice. It is worth to mention that the formation of Cu(II) and ATO complex inside the liposomal inner aqueous phase in the loading process provided the main basis for high drug encapsulation, and extended *in vivo* circulation of encapsulated ATO. On the other hand, the $Cu(OAc)_2$ gradient based remote loading method provided a feasible strategy for co-administration of ATO and Cu(II) for improving antitumor efficacy of ATO, which may find potential applications in the treatment of various tumors.

Conflicts of interest

The authors declare no conflict of interest.

Acknowledgments

This work was supported by Research Grant from Liaoning Province Office of Education, China (No. L2014395), the Natural Science Foundation of Liaoning Province (No. 201602711), and Supporting Program for Young Researchers from Sheyang Pharmaceutical University.

REFERENCES

[1] Emadi A, Gore SD. Arsenic trioxide - An old drug rediscovered. Blood Rev 2010;24(4–5):191–9.
[2] Gill H, Yim R, Lee HKK, Mak V, Lin SY, Kho B, et al. Long-term outcome of relapsed acute promyelocytic leukemia treated with oral arsenic trioxide-based reinduction and maintenance regimens: A 15-year prospective study. Cancer 2018;124(11):2316–26.
[3] Hoonjan M, Jadhav V, Bhatt P. Arsenic trioxide: Insights into its evolution to an anticancer agent. J Biol Inorg Chem 2018;23(3):313–29.
[4] Khairul I, Wang QQ, Jiang YH, Wang C, Naranmandure H. Metabolism, toxicity and anticancer activities of arsenic compounds. Oncotarget 2017;8(14):23905–26.
[5] Murgo AJ. Clinical trials of arsenic trioxide in hematologic and solid tumors: Overview of the National Cancer Institute cooperative research and development studies. Oncologist 2001;6(Suppl 2):22–8.
[6] Maeda H, Hori S, Ohizumi H, Segawa T, Kakehi Y, Ogawa O, Kakizuka A. Effective treatment of advanced solid tumors by the combination of arsenic trioxide and L-buthionine-sulfoximine. Cell Death Differ 2004;11(7):737–46.
[7] Bael TE, Peterson BL, Gollob JA. Phase II trial of arsenic trioxide and ascorbic acid with temozolomide in patients with metastatic melanoma with or without central nervous system metastases. Melanoma Res 2008;18(2):147–51.
[8] Westervelt P, Pollock J, Haug J, Ley TJ, Dipersio JF. Response and toxicity associated with dose escalation of arsenic trioxide in the treatment of resistant acute promyelocytic leukemia. Blood 1997;90(Suppl 1):249b.
[9] Noble GT, Stefanick JF, Ashley JD, Kiziltepe T, Bilgicer B. Ligand-targeted liposome design: Challenges and fundamental considerations. Trends Biotechnol 2014;32(1):32–45.
[10] Hu CM, Aryal S, Zhang L. Nanoparticle-assisted combination therapies for effective cancer treatment. Ther Deliv 2010;1(2):323–34.
[11] Kallinteri P, Fatouros D, Klepetsanis P, Antimisiaris SG. Arsenic trioxide liposomes: Encapsulation efficiency and *in vitro* stability. J Liposome Res 2004;14(1–2):27–38.
[12] Maurer N, Wong KF, Hope MJ, Cullis PR. Anomalous solubility behavior of the antibiotic ciprofloxacin encapsulated in liposomes: A 1H-NMR study. Biochim Biophys Acta 2012;1374(1–2):9–20.
[13] Fenske DB, Wong KF, Maurer E, Maurer N, Johanna M, Nancy B, et al. Ionophore-mediated uptake of ciprofloxacin and vincristine into large unilamellar vesicles exhibiting transmembrane ion gradients. Biochim Biophys Acta 1998;1414(1–2):188–204.
[14] Gubernator J. Active methods of drug loading into liposomes: Recent strategies for stable drug entrapment and increased *in vivo* activity. Expert Opin Drug Deliv 2011;8(5):565–80.
[15] Taggar AS, Alnajim J, Anantha M, Tomas A, Webb M, Ramsay E, et al. Copper-topotecan complexation mediates drug accumulation into liposomes. J Control Rel 2006;114(1):78–88.
[16] Cui J, Li CL, Wang LF, Wang CX, Yang H, Li YH, et al. Ni^{2+}-mediated mitoxantrone encapsulation: Improved efficacy of fast release formulation. Int J Pharm 2009;368(1–2):24–30.
[17] Akhtar A, Wang SX, Ghali L, Bell C, Wen X. Recent advances in arsenic trioxide encapsulated nanoparticlesas drug delivery agents to solid cancers. J Biomed Res 2017;31(3):177–88.
[18] Ahn RW, Barrett SL, Raja MR, Jennifer KJ, Lidia S, Haimei C, et al. Nano-encapsulation of arsenic trioxide enhances murine lymphoma model while minimizing its impact on ovarian reserve *in vitro* and *in vivo*. PLoS One 2013;8(3):e58491.
[19] Richard WA, Feng C, Haimei C, Stephen TS, Jeffrey DC, Anil KP, et al. A novel nanoparticulate formulation of arsenic trioxide with enhanced therapeutic efficacy in a murine model of breast cancer. Clin Cancer Res 2010;16(14):3607–17.
[20] Wang Y, Zeng S, Lin TM, Krugner-Higby L, Lyman D, Steffen D, et al. Evaluating the anticancer properties of liposomal copper in a nude xenograft mouse model of human prostate cancer: Formulation, *in vitro*, *in vivo*, histology and tissue distribution studies. Pharm Res 2014;31(11):3106–19.
[21] Safi R, Nelson ER, Chitneni SK, Franz KJ, George DJ, Zalutsky MR, et al. Copper signaling axis as a target for prostate cancer therapeutics. Cancer Res 2014;74(20):5819–31.
[22] Lun X, Wells JC, Grinshtein N, King JC, Hao XG, Dang NH, et al. Disulfiram when combined with copper enhances the therapeutic effects of temozolomide for the treatment of Glioblastoma. Clin Cancer Res 2016;22(15):3860–75.
[23] Denoyer D, Masaldan S, La Fontaine S, Cater MA. Targeting copper in cancer therapy: 'Copper that cancer'. Metallomics 2015;7(11):1459–76.
[24] Zhou Z, Zhang D, Yang L, Ma PT, Si YN, Kortz U, et al. Nona-copper(II)-containing 18-tungsto-8-arsenate(III) exhibits antitumor activity. Chem Commun 2013;49(35):5189–91 (Camb).
[25] Ngoune R, Contini C, Hoffmann MM, von Elverfeldt D, Winkler K, Putz G. Optimizing antitumor efficacy and adverse effects of pegylated liposomal doxorubicin by scheduled plasmapheresis: Impact of timing and dosing. Curr Drug Deliv 2018;15(9):1261–70.

[26] Sun J, Song Y, Lu M, Lin XY, Liu Y, Zhou SL, et al. Evaluation of the antitumor effect of dexamethasone palmitate and doxorubicin co-loaded liposomes modified with a sialic acid–octadecylamine conjugate. Eur J Pharm Sci 2016;93:177–83.
[27] Subbarayan PR, Ardalan B. In the war against solid tumors arsenic trioxide needs partners. J Gastrointest Cancer 2014;45(3):363–71.
[28] Agrahari V. Facilitating the translation of nanomedicines to a clinical product: challenges and opportunities. Drug Discov Today 2018;23(5):974–91.
[29] Chen H, Macdonald RC, Li S, Krett NL, Rosen ST, Ohalloran TV. Lipid encapsulation of arsenic trioxide attenuates cytotoxicity and allows for controlled anticancer drug release. J Am Chem Soc 2006;128(41):13348–9.
[30] Wang H, Zhu W, Liu J, Dong Z, Liu Z. pH-responsive nanoscale covalent organic polymers as a biodegradable drug carrier for combined photodynamic chemotherapy of cancer. ACS Appl Mater Interfaces 2018;10(17):14475–82.
[31] Oku N. Innovations in liposomal DDS technology and its application for the treatment of various diseases. Biol Pharm Bull 2017;40(2):119–27.